Journal of Peptide Science
J. Pept. Sci. 2008; **14**: 890–897
Published online 20 February 2008 in Wiley InterScience (www.interscience.wiley.com). DOI: 10.1002/psc.1020

JOURNAL OF PEPTIDE SCIENCE

Mutations on *N*-terminal region of Taiwan cobra phospholipase A_2 result in structurally distorted effects

YI-LING CHIOU,[a] SHINNE-REN LIN[b] and LONG-SEN CHANG[a]*

[a] Institute of Biomedical Sciences, National Sun Yat-Sen University-Kaohsiung Medical University Joint Research Center, National Sun Yat-Sen University, Kaohsiung 804, Taiwan
[b] Department of Medicinal and Applied Chemistry, Kaohsiung Medical University, Kaohsiung 807, Taiwan

Received 1 November 2007; *Revised 13 December 2007*; *Accepted 20 December 2007*

Abstract: In the present study, three Taiwan cobra PLA_2 variants were prepared by adding an extra *N*-terminal Met, substituting Asn-1 by Met or deleting the *N*-terminal heptapeptide. Recombinant PLA_2 mutants were expressed in *Escherichia coli* (*E. coli*), and purified to homogeneity by reverse phase HPLC. Fluorescence measurement showed that the hydrophobic character of the catalytic site, the microenvironment of Trp residues and energy transfer from excited Trp to 8-anilinonaphthalene sulfonate (ANS) were affected by *N*-terminal mutations. An alteration in the structural flexibility of the active site was noted with the mutants lacking the *N*-terminal heptapeptide or with an extra *N*-terminal Met added as evidenced by the inability of the two variants to bind with Ba^{2+}. Moreover, modification of Lys residues and energy transfer within the protein-ANS complex revealed that the Ca^{2+}-induced change in the global structure of PLA_2 was different from that in *N*-terminal variants. Together with the fact that an 'activation network' connects the *N*-terminus with the active site, our data suggest that mutagenesis on the *N*-terminal region affects directly the fine structure of the catalytic site, which subsequently transmits its influence in altering the structure outside the active site of PLA_2. Copyright © 2008 European Peptide Society and John Wiley & Sons, Ltd.

Keywords: phospholipase A_2; *N*-terminal mutation; catalytic site; Trp fluorescence; energy transfer; interfacial binding site

INTRODUCTION

The phospholipase A_2 (PLA_2) enzymes catalyze specifically the hydrolysis of fatty acid bonds at the position 2 of 1,2-diacyl-*sn*-phosphoglycerides in the presence of Ca^{2+} [1]. Although PLA_2 enzymes hydrolyze monomeric substrates, their activities increase substantially by several orders of magnitude when the substrates are in aggregated form. This result has led to the proposition that there is a specific interfacial recognition site at the *N*-terminal region with specific affinity for lipid–water interfaces [1]. Qin *et al.* [2] suggested that the *N*-terminal region of PLA_2 enzymes acts as a regulatory domain that mediates interfacial activation of these enzymes. Moreover, several lines of evidence showed that the *N*-terminal region contributes functionally to facilitate a productive-mode orientation of PLA_2 at the membrane surface [2,3]. Alternatively, Tatulian [4] proposed that an allosteric coupling between the membrane-binding site and the catalytic center of PLA_2 is related to the interfacial activation of the enzyme. This is consistent with the studies on the tertiary structure of *Naja naja atra* PLA_2, showing that the hydrogen-bonding network that connects the active site with the *N*-terminus is an 'activation network' and stabilizes the productive conformation of PLA_2 for aggregate substrates [5,6]. These observations suggest that the integrity of *N*-terminal region is important for maintaining the active conformation of PLA_2 enzymes. Alternatively, Ca^{2+} binds at the catalytic site and is an essential cofactor for the catalytic activity of PLA_2 enzymes [1]. Moreover, it was found that Ca^{2+} enhanced the structural stability of PLA_2 [7]. These reflect that the active site launches its structural influence on the remaining portion of the enzymes. The finding that modification of bovine pancreas PLA_2 and *Agkistrodon halys* PLA_2 by *p*-bromophenacyl bromide led to conformational changes outside the catalytic site [8,9] supports this proposition. Noticeably, Anderson *et al.* [10] noted that Ba^{2+}, Eu^{3+}, Tb^{3+}, and Gd^{3+} could bind at the Ca^{2+}-binding site of porcine pancreatic PLA_2, but only Gd^{3+} supported catalytic activity. Likewise, fluorescence measurement showed that the structure of *N. naja atra* PLA_2 is perturbed by the binding of Ca^{2+}, Sr^{2+} and Ba^{2+}, but Sr^{2+} and Ba^{2+} are inhibitor ions of PLA_2 [11]. These results imply that the fine structure of catalytic site within the PLA_2 molecule is rather flexible, thus allowing it to accommodate metal ions with varying sizes. In order to elucidate the contribution of *N*-terminal region in maintaining the structure of the active site and the global conformation of PLA_2 enzymes, analyses on the *N*-terminally mutated *N. naja atra* PLA_2 are carried out in the present study.

MATERIALS AND METHODS

PLA_2 was isolated from the venom of *N. naja atra* (Taiwan cobra) according to the procedure as previously described

* Correspondence to: Long-Sen Chang, Institute of Biomedical Sciences, National Sun Yat-Sen University, Kaohsiung 804, Taiwan;
e-mail: lschang@mail.nsysu.edu.tw

[12]. Acrylamide, 8-anilinonaphthalene sulfonate (ANS), 5,5′-dithio-bis-(2-nitrobenzoic acid), egg yolk phosphatidylcholine (Type X-E) and trinitrobenzene sulfonate (TNBS) were purchased from Sigma-Aldrich Inc., and SynChropak RP-P column (4.6 mm × 25 cm) was obtained from SynChrom Inc (Lafayette, IN, USA). 2-Nitro-5-thiosulfobenzoate (NTSB) was synthesized from 5,5′-dithio-bis-(2-nitrobenzoic acid) according to the procedure of Thannhauser and Scheraga [13]. Unless otherwise specified, all other reagents were of analytical grade.

PCR Amplification and Cloning

Cellular RNA was isolated from the snake *(N. naja atra)* venom glands as described in Chang *et al.* [14]. Two oligonucleotide primers of sense and antisense orientations according to the signal peptide and 3′-noncoding region of *N. naja atra* PLA_2 cDNA (accession no. X73 225) with the forward sequence 5′-GACTCCTGCTCACCTTCTGATCCTG-3′ and the reverse sequence 5′-CCTCTCAAATATCATTGGCAACGTGC-3′ were synthesized.

RT-PCR was performed according to the procedure described in Chang *et al.* [14]. The PCR products were cloned into a pCRII vector according to the TA-cloning procedures (Invitrogen, San Diego, USA).

Construction of Expression Vector Containing Wild-type or Mutated PLA_2cDNAs

Synthetic oligonucleotides were designed to produce a 377-bp amplified DNA fragment spanning the open-reading frame of the PLA_2. Primer 1 introduced a 5′ *Nde* I site and an in-frame initiating Met codon preceding Asn-1,5′-GATATGAACCTCTATCAGTTTAAAAACATGATTC-3′ (The *Nde* I site was indicated by underline). Primer 2 was the reverse primer for RT-PCR amplification. The PCR products were cloned into pCR II vector, and the inserted DNA fragment was then ligated into the large fragment of *Nde* I/*EcoR* I-cut pET22b(+). Two sense primers, 5′-CATATGCTCTACCAGTTCAAAAACATGATTCAATG-3′(N1M) and 5′-CATATGATTCAATGTACCGTCCCCAGTCGA-3′(ΔN7), were employed to prepare PLA_2(N1M) and PLA_2(ΔN7) cDNAs, respectively. The entire sequence was confirmed by dideoxynucleotide sequencing.

The resulting plasmid was transformed into *Escherichia coli* [*E. coli* strain BL21(DE3)]. For induction of gene expression, *E. coli* BL21(DE3) cells harboring the expression plasmid were grown at 37 °C in LB medium containing 50 μg/ml ampicillin. After reaching an $OD_{550} = 1.0$, isopropyl-β-D-thiogalactoside was added to a final concentration of 1 mM. The culture was induced for a period of up to 4 h. The cells were harvested and lysed by ultrasonication.

Preparation of Recombinant PLA_2

Recombinant PLA_2 was isolated from the inclusion bodies of *E. coli*, and the proteins were refolded using NTSB reagent according to the procedure described by Chang *et al.* [15]. The recombinant PLA_2 was further purified by HPLC on a SynChropak RP-P column (4.6 mm × 25 cm), equilibrated with 0.1% trifluoroacetic acid and eluted with a linear gradient of 25–50% acetonitrile for 70 min. The eluent was monitored at 235 nm.

Acrylamide Quenching Measurement

Quenching Trp fluorescence was studied according to the method described by Eftink and Ghiron [16]. Fluorescence intensity was measured by a Hitachi model 4500 spectrophotofluorometer using a 5-nm slit width. An excitation wavelength at 295 nm was employed to ensure selective excitation of the Trp residue. For all quenching experiments, the absorbance of samples at 295 nm was always ≤0.06 and thus no correction for inner effects was necessary. The shape and position of the emission spectra were not altered by the addition of the quenching agent. Therefore, the fluorescence intensity was monitored at the emission maximum, and quenched by the progressive addition of small aliquots of acrylamide to the 1-cm fluorescence cuvettes. Data were corrected for dilution due to the addition of a titrant. All solutions were protected from light and used promptly after preparation. The solution was equilibrated at 30 °C before and during the measurements.

For a simple, single fluorophore or homogeneous system, fluorescence quenching was analyzed according to the Stern–Volmer equation: $Fo/F = 1 + \mathrm{Ksv}[Q]$ where Fo is the fluorescence in the absence of quencher, F is the fluorescence at molar quencher concentration $[Q]$, and Ksv is the Stern–Volmer quenching constant obtained from the slope of a plot of Fo/F *versus* $[Q]$.

Fluorescence Measurement

Fluorescence intensity was measured by a Hitachi model 4500 spectrophotofluorometer using a 5-nm slit width. All measurements used a 1-cm path length and were performed in a total volume of 2 ml of 0.025 M Tris-0.1 M NaCl (pH 8.0) which was kept at 30 °C by circulating water through the cell holder. An excitation wavelength at 360 nm was employed to selectively excite the ANS molecule. Fluorescence emission was monitored at the wavelength of maximum intensity. Titrations with divalent cations (Ca^{2+}, Sr^{2+}, or Ba^{2+}) were made manually by the addition of small aliquots of a concentrated divalent cation solution to a solution of protein–ANS complexes. Dilutions on addition of divalent cations never exceeded 5% of the starting volume. Measurements were taken at equilibrium, which in these studies were taken to be a fluorescence measurement that remained constant over time. In the titration of protein with divalent cations (M^{2+}), a plot of change in ANS fluorescence intensity ΔF *versus* $\Delta F/[M^{2+}]$ gave lines with a slope corresponding to the dissociation constant, K_d, of the enzyme molecule for M^{2+} [11].

Quenching of Trp fluorescence upon addition of ANS was analyzed according to the equation, $Fo - F = (Fo - Fi) - K_{dapp}(Fo - F)/[\mathrm{ANS}]$, where Fo and F denote the observed fluorescence in the absence and presence of the ANS, respectively; and Fi is the fluorescence at infinite concentration of ANS. A plot of $Fo - F$ *versus* $(Fo - F)/[\mathrm{ANS}]$ yielded a straight line whose slope equaled K_{dapp} of ANS [17].

Modification of Amino Groups with TNBS

PLA_2 (2 mg) in 2 ml of 0.05 M borate buffer (pH 8.6) was incubated with three-fold molar excess of TNBS. The reaction was allowed to proceed at 30 °C for 30 min and the mixture was desalted by passage through a Sephadex G-25 column. The

DOI: 10.1002/psc

trinitrophenylated (TNP) proteins were separated by reverse phase HPLC on a SynChropak RP-P column (4.6 mm × 25 cm), equilibrated with 0.1% trifluoroacetic acid and eluted with a linear gradient of 25–60% acetonitrile for 70 min. The eluent was monitored at 235 nm.

Other Tests

Determination of PLA_2 activity, CD measurement, SDS-PAGE, and native gel electrophoresis were performed in essentially the same manner as previously described [7,12,14].

RESULTS AND DISCUSSION

Three *N*-terminally mutated PLA_2s, designated as M-PLA_2, PLA_2(N1M) and PLA_2(ΔN7), were prepared in the present study. M-PLA_2 contained an extra Met preceding Asn-1 of native PLA_2, and Asn-1 was substituted by Met-1 in PLA_2(N1M). Alternatively, PLA_2(ΔN7) was deprived of the *N*-terminal heptapeptide of PLA_2. The expressed PLA_2s appeared exclusively in the inclusion bodies of *E. coli*, and thus refolding of the recombinant proteins was carried out to obtain folded proteins. As shown in Figure 1, the refolded PLA_2 mutants were purified by HPLC on a SynChropak RP-P column. The homogeneity of mutated PLA_2s was further verified by SDS-PAGE (Figure 1). Mass analyses showed that PLA_2 mutants had the molecular sizes corresponding to those calculated from their amino acid sequence (data not shown). The enzymatic activity of M-PLA_2, PLA_2(N1M), and PLA_2(ΔN7) was approximately 3.6, 5.3, and 0.6% of that of native PLA_2. This was in line with the results of previous studies (Yang and Chang, 1988) showing that the intact *N*-terminal region was essential for the enzymatic activity of PLA_2. In order to confirm that the refolding process was effectively conducted, native PLA_2 was labeled with NTSB and then refolded according to the same procedure for refolding of mutated PLA_2. As shown in the insert B of Figure 1, native gel electrophoresis analyses revealed that the refolded PLA_2 exhibited electrophoretic mobility indistinguishable from that of native PLA_2. Moreover, using egg yolk phosphatidylcholine as substrate, PLA_2 and refolded PLA_2 showed a specific activity of 369 ± 5 units/mg and 367 ± 6 units/mg, respectively.

N. naja atra PLA_2 contains three Trp residues at positions 18, 19, and 61. Chemical modification and mutagenesis studies revealed that the three Trp residues were located at lipid–water interface for catalytic action [18,19]. Thus, the changes in fluorescent properties of Trp residues resulting from mutations should enable us to explore the dynamic changes at the interfacial site of PLA_2. As shown in Figure 2(A), the intrinsic fluorescence of PLA_2 mutants decreased markedly, reflecting that the microenvironment of Trp residues in mutants was altered. Fluorescence quenching studies revealed that the Trp residues in PLA_2(ΔN7) had a decreased

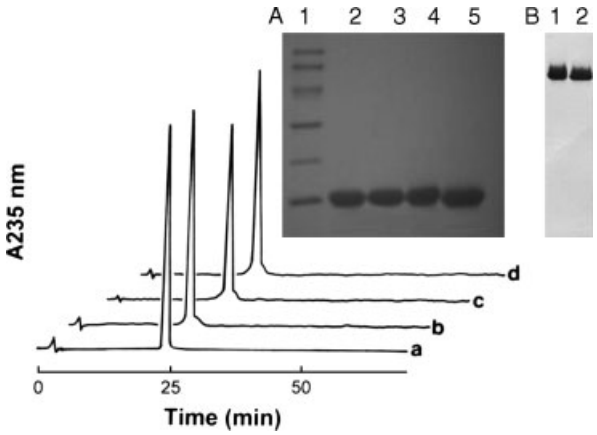

Figure 1 Purification of PLA_2 mutants by reverse phase HPLC. Samples were applied on a SynChropak RP-P column (4.6 mm × 25 cm) equilibrated with 0.1% trifluoroacetic acid and eluted with a linear gradient of 25–50% acetonitrile for 70 min. Lines a, b, c, and d represent the chromatographic profiles of native PLA_2, M-PLA_2, PLA_2(N1M) and PLA_2(ΔN7), respectively. Flow rate was 0.8 ml/min and the effluent was monitored at 235 nm. Insert A: SDS-PAGE analyses of purified PLA_2 and mutants. Lane 1, molecular markers (phosphorylase b, 97 KDa; albumin, 66 KDa; ovalbumin, 45 KDa; carbonic anhydrase, 30 KDa; trypsin inhibitor, 20.1 KDa; α-lactalbumin, 14.4 KDa); Lane 2, PLA_2; Lane 3, M-PLA_2; Lane 4, PLA_2(N1M); Lane 5, PLA_2(ΔN7). Insert B: native gel electrophoresis analyses of PLA_2 and refolded PLA_2; Lane 1, PLA_2; Lane 2, refolded PLA_2.

accessibility for acrylamide compared with those of PLA_2. This revealed that the degree of exposure of Trp residues changed after removal of *N*-terminal heptapeptide. Alternatively, the susceptibility of Trp residues in M-PLA_2 and PLA_2(N1M) was similar to that in native enzyme.

ANS has been used extensively as an extrinsic fluorescent probe to monitor conformational changes in biological macromolecules [17,20,21]. In contrast to the weak green fluorescence of ANS in aqueous solutions, an intensive blue fluorescence is exhibited when ANS dissolves in nonpolar solvents or when ANS binds in biological macromolecules. A decreased polarity of the probe's environment is thought to be the main factor contributing to the observed fluorescence enhancement upon binding of ANS to a protein [22]. Previous studies suggested that the hydrophobic pocket of *N. naja atra* PLA_2 that binds with ANS is the site at which PLA_2 interacts with a substrate [23]. Moreover, modification of catalytic residue His-47 in *N. naja atra* PLA_2 is inhibited by the binding of ANS [24]. Thus, the change in the ability to enhance ANS fluorescence indicates an alteration in the fine structure of the catalytic site. As shown in Figure 3(A), compared with PLA_2, PLA_2 mutants had a marked decrease in the enhancement of ANS fluorescence intensity, suggesting that mutations on the *N*-terminal region might perturb the structure of the catalytic site.

DOI: 10.1002/psc

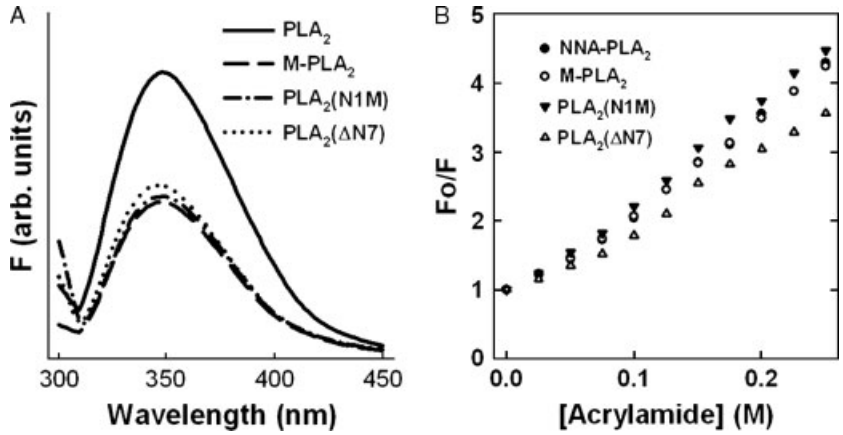

Figure 2 Fluorescence emission spectra and acrylamide quenching of Trp fluorescence of PLA_2 and its mutants. The sample cuvettes contained 7.5 μM of protein in 0.025 M Tris-0.1 M NaCl (pH 8.0). (A) Fluorescence emission spectra of native and mutated PLA_2s at an excitation wavelength of 295 nm. (B) Acrylamide quenching of PLA_2 and its mutants.

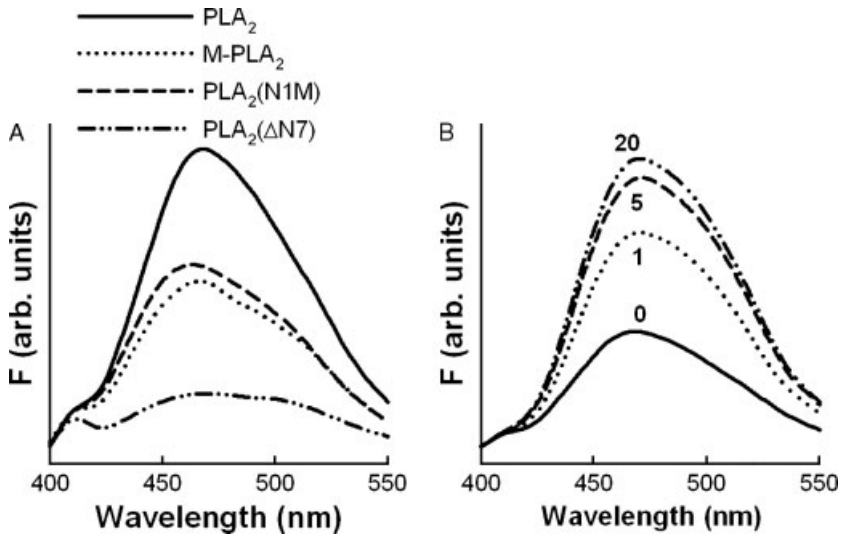

Figure 3 Fluorescence emission spectra of PLA_2–ANS complexes and mutated PLA_2–ANS complexes. (A) Enhancement of ANS fluorescence by PLA_2 and its mutants. The sample cuvettes contained 7.5 μM of proteins/ml of 0.025 M Tris-0.1 M NaCl (pH 8.0) and 7.5 μM ANS. (B) Ca^{2+} enhanced the ANS fluorescence of PLA_2–ANS complexes. The sample cuvettes contained 7.5 μM of PLA_2/ml of 0.025 M Tris-0.1 M NaCl (pH 8.0) and 7.5 μM ANS in the presence of various concentrations of Ca^{2+} (mM) as indicated.

As illustrated in Figure 3(B), the emission intensity of PLA_2–ANS complexes increased in parallel with increasing concentration of Ca^{2+} until the saturation level was reached. Likewise, the addition of Sr^{2+} and Ba^{2+} into the PLA_2–ANS complexes solution also resulted in a marked enhancement of ANS fluorescence. Since the binding of divalent cations (M^{2+}) is associated with a marked increase in the fluorescence of the ANS-enzyme complexes, the M^{2+}-enzyme interaction can be monitored by the change in intensity of the ANS-enzyme complexes caused by the addition of M^{2+}. The binding affinities of PLA_2 for divalent cations were determined from a plot of ΔF *versus* $\Delta F/[M^{2+}]$, showing that the affinities (K_d) of PLA_2 for Ca^{2+}, Sr^{2+}, and Ba^{2+} were 0.76, 0.69, and 0.56 mM, respectively. Alternatively, the Ca^{2+}-binding affinities (K_d) of M-PLA_2, PLA_2(N1M), and PLA_2(ΔN7) were 1.26, 2.06, and 1.98 mM, respectively (Table 1). Apparently, *N*-terminally mutated PLA_2 still retained the Ca^{2+}-binding ability. Although *N*-terminal mutants showed a Sr^{2+}-binding ability, the Ba^{2+}-binding capability of M-PLA_2 and PLA_2(ΔN7) could not be detected owing to a marginal change in the ANS fluorescence when the mutants were titrated with Ba^{2+}. Because the *N*-terminal mutants still retained the ANS-binding capability (Figure 3(A)), the structural flexibility with the active site of PLA_2 for accommodating metal ions of varying sizes was altered by adding an extra *N*-terminal Met or removal of an *N*-terminal heptapeptide.

The emission spectra resulting from excitation at 295 nm of PLA_2–ANS complexes are shown in Figure 4. In the absence of ANS, a fluorescence

DOI: 10.1002/psc

Table 1 Metal-binding properties of PLA_2 and its mutants

	K_d for Ca^{2+} (mM)	K_d for Sr^{2+} (mM)	K_d for Ba^{2+} (mM)
PLA_2	0.76	0.69	0.56
M-PLA_2	1.26	1.94	N.D.[a]
PLA_2(N1M)	2.06	1.73	2.01
PLA_2(ΔN7)	1.98	5.16	N.D.[a]

[a] Enhancement of ANS fluorescence intensity is too small to accurately determine the binding constant for Ba^{2+}.

emitted maximally at 350 nm from the excitation of Trp residues of PLA_2 was noted (Figure 2). The emission was quenched on the addition of ANS, and a second emission at 470 nm was a composite of the fluorescence of the PLA_2–ANS complexes. The Trp emission at 350 nm decreased and the emission intensity of ANS increased upon further raising the ANS concentration. These spectral changes were indicative of the transfer of energy from a chromophore inherent in the protein to an absorbed molecule (ANS). The ANS concentration-dependent energy transfer from excited Trp to ANS was observed for PLA_2 and its mutants (Figure 4). Compared with that of PLA_2 and PLA_2(N1M), ANS fluorescence of M-PLA_2 and PLA_2(ΔN7) were weakly enhanced.

The quenching of Trp fluorescence upon addition of ANS was analyzed according to the equation, $(Fo - F) = (Fo - Fi) - K_{dapp}(Fo - F)/[ANS]$. A plot of $Fo - F$ *versus* $(Fo - F)/[ANS]$ yielded a straight line whose slope equaled K_{dapp} of ANS (Figure 5). This K_{dapp} was proportional to the efficiency of the energy transfer from excited Trp to ANS molecule. The K_{dapp} for ANS of PLA_2, M-PLA_2, PLA_2(N1M), and PLA_2(ΔN7) were 96, 93.8, 116.0, and 60.5 μM, respectively. Alternatively, in the presence of Ca^{2+}, the K_{dapp} for ANS were 63.8, 123.0, 64.3, and 121.0 μM, respectively. This indicated that Ca^{2+} enhanced the energy transfer in PLA_2 and PLA_2(N1M), but a reversed effect was noted with M-PLA_2 and PLA_2(ΔN7). Campbell and Dwek [25] and Lacowicz [26] suggested that the resonance energy transfer in terms of a dipole–dipole interaction between the donor and acceptor pair depends on $1/R^6$, where R is the intermolecule distance. In a general case, the distance between the donor (Trp residues) and acceptor (ANS) can vary both as a result of a range of distance and by diffusion. Thus, our data indicated that the spatial distance between Trp residues and the active site in PLA_2 was not the same as that in *N*-terminal mutants, and altered differently in response to the binding of Ca^{2+}.

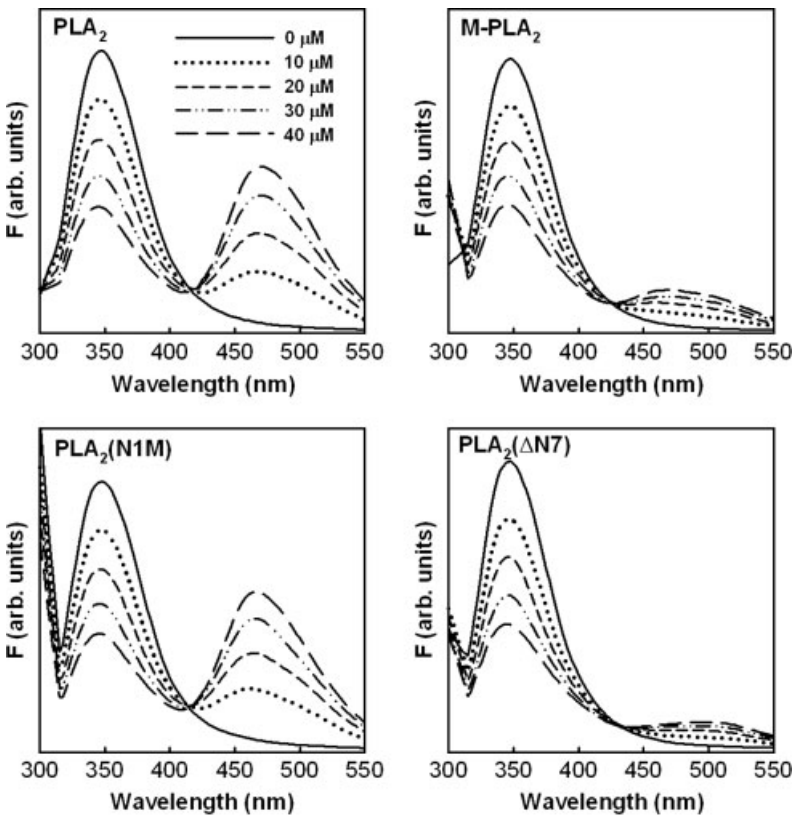

Figure 4 Energy transfer from excited Trp to ANS molecule in native and mutated PLA_2s. Protein concentration of 7.5 μM in 0.025 M Tris-0.1 M NaCl (pH 8.0) was used in the experiments. The excitation wavelength was 295 nm. The addition of indicated ANS concentration caused a decrease in the Trp fluorescence with an enhancement of ANS fluorescence.

DOI: 10.1002/psc

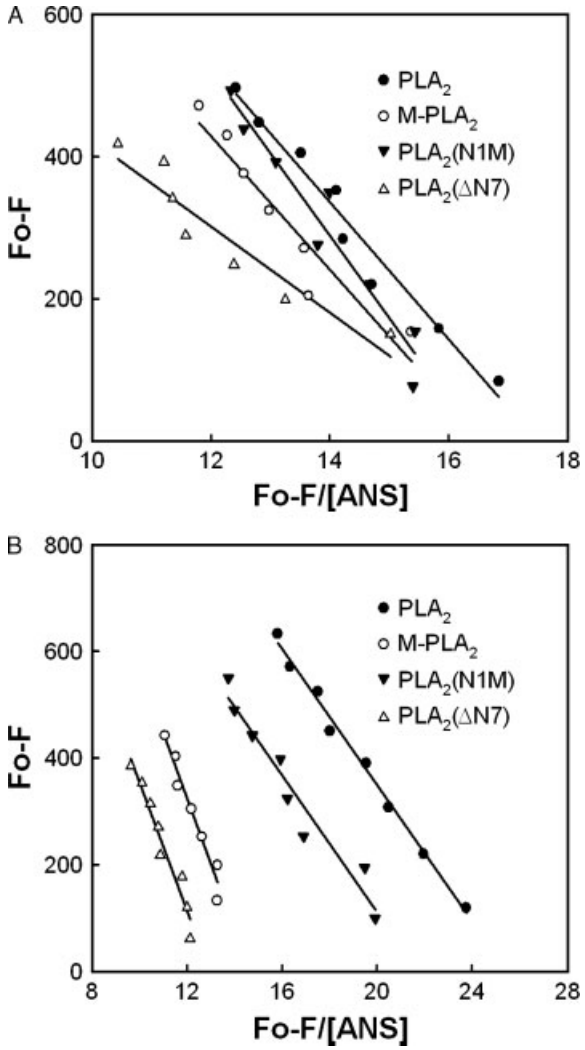

Figure 5 Estimation of apparent dissociation constants (K_{dapp}) for ANS from the decrease in Trp fluorescence of PLA_2 and its mutants in the absence and presence of 5 mM Ca^{2+}. The sample cuvettes contained 7.5 μM protein in 0.025 M Tris-0.1 M NaCl (pH 8.0) without (A) or with (B) 5 mM Ca^{2+} during the titration of ANS. The excitation wavelength was 295 nm, and the emission maximum at 345 nm was measured. A plot of $Fo - F$ *versus* $(Fo - F)$/[ANS] yielded a straight line whose slope equaled the K_{dapp} of ANS.

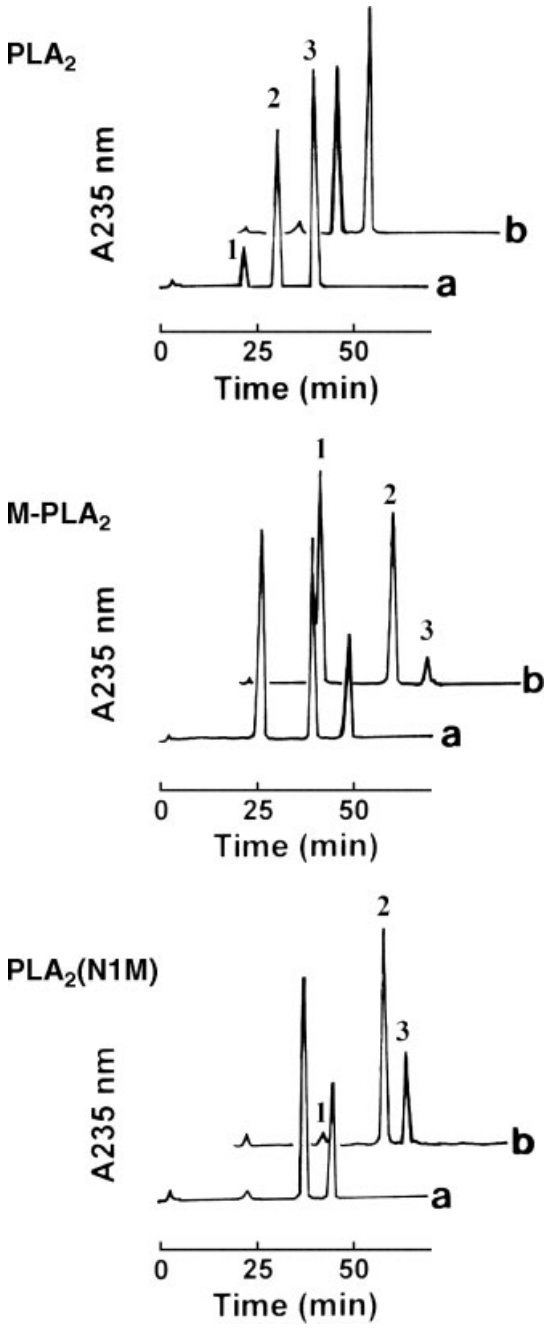

Figure 6 Chemical modification of Lys-6 and Lys-65 in PLA_2 and its mutants with TNBS. Chemical modification of Lys-6 and Lys-65 with TNBS was carried out in the absence (line a) or presence (line b) of 5 mM Ca^{2+}. Samples of TNP proteins were applied on a SynChropak RP-P column (4.6 mm × 25 cm) equilibrated with 0.1% trifluoroacetic acid and eluted with a linear gradient of 25–60% acetonitrile for 70 min. Flow rate was 0.8 ml/min and the effluent was monitored at 235 nm. Peaks 1, 2, and 3 represent unmodified protein, TNP-1 and TNP-2, respectively. TNP-1 contained only one TNP group on Lys-6, and both Lys-6 and Lys-65 were modified in TNP-2.

This reflected a change in the global structure with PLA_2 variants. Compared with that of PLA_2, CD spectra of PLA_2 mutants showed a decreased negative ellipticity (data not shown). This again emphasized that the gross conformation of PLA_2 and *N*-terminally mutated PLA_2s differed.

X-ray crystallographic analyses show that, in addition to Trp-18, the residues Leu-2, Tyr-3, Lys-6, Ile-9, Arg-30, and Tyr-68 constitute the hydrophobic channel involved in the interaction of enzyme molecule with phospholipids/substrate [5]. The structural perturbation with *N*-terminal variants was further assessed by modification of Lys-6 with TNBS. As shown in Figure 6, two TNP derivatives of PLA_2 were separated by HPLC. Our previous results revealed that the TNP derivative at peak 2 contained a modified Lys-6, and both Lys-6 and Lys-65 were modified in the TNP derivative at peak 3 [27]. Figure 6 showed that Ca^{2+} enhanced

DOI: 10.1002/psc

the reactivity of Lys-6 and Lys-65 in PLA_2 toward TNBS. Unlike native PLA_2, Ca^{2+}-enhanced effect was inappreciably noted for trinitrophenylation of PLA_2(N1M). In the meantime, trinitrophenylation of M-PLA_2 was reduced by the addition of Ca^{2+}. Apparently, in addition to the substrate-binding site of neighboring Lys-6, mutations on the *N*-terminal region also affected the structure around Lys-65. Lys-6 was deleted in PLA_2(ΔN7), and thus modification of the mutated PLA_2 could not reveal the conformational event with Lys-6. Nevertheless, it was found that trinitrophenylation of Lys-65 in PLA_2(ΔN7) was insignificantly changed by the Ca^{2+} (data not shown).

Previous studies show that the *N*-terminal segment of PLA_2 is involved in discrimination of different substrates and inhibitors [28,29]. Studies on the chimeric PLA_2 find that the *N*-terminal region with the same amino acid sequence interacts differently with the remaining portion of PLA_2 [2]. Moreover, the chimeric PLA_2 displays a decreased enzymatic activity and phospholipid-binding affinity. Alternatively, it is found that structurally distinct PLA_2 enzymes interact differentially with phospholipids for performing their catalytic function in a different manner [30]. These results reflect that, in addition to the substrate-binding site, interfacial activation should result in an alteration in the fine structure of the catalytic site as well as the global conformation of PLA_2 enzymes. Inspection of the helical wheel plot for the *N*-terminal region of PLA_2 (Figure 7) shows distinct hydrophobic and hydrophilic faces. Difference in the extent of trinitrophenylated Lys-6 reflects that the side chains in the *N*-terminal α-helical structure should adopt different orientations between PLA_2 and its mutants. Given that a hydrogen-bonding network connects the *N*-terminus with the active site [5,6], one could imagine that, using the hydrogen-bonding network as axis, active site-bound Ca^{2+} induces the rotation of *N*-terminal helical wheel to expose the residues that bind with phospholipids/substrate. Trinitrophenylation of Lys residues reveals that Ca^{2+}-induced productive conformation with native PLA_2 does not occur well with the *N*-terminal mutants. The effect of Ca^{2+} on the energy transfer within the protein–ANS complex again supports this notion. Findings of the change in the microenvironment of Trp residues and the energy transfer from excited Trp to ANS with PLA_2 variants suggest that mutations on the *N*-terminal region also affect the structure at lipid–water interfaces. In addition to the hydrophobic character of the active site, the structural flexibility of the catalytic site in mutated PLA_2s is altered as evidenced by their ability to bind with Ca^{2+}, Sr^{2+} and Ba^{2+}. Collectively, our data indicate that mutagenesis on the *N*-terminal region affects the fine structure of the catalytic site, which transmits subsequently its influence in altering the structure outside the active site of PLA_2.

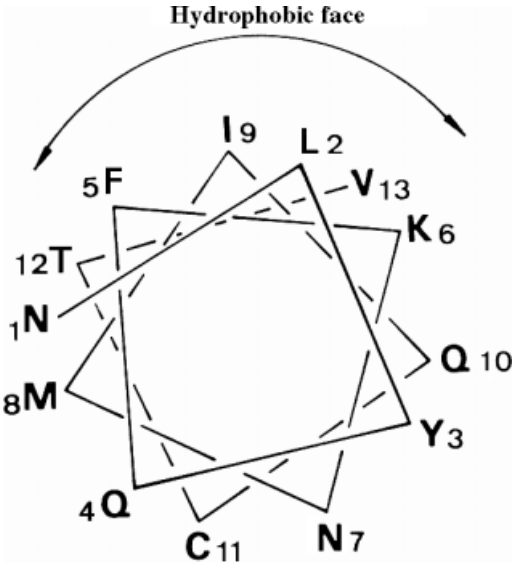

Figure 7 Helical wheel plot of *N*-terminal region of PLA_2. The *N*-terminal region of PLA_2 is an α-helical structure as revealed by the three-dimensional structure of *N. naja atra* PLA_2 [5]. Leu-2, Phe-5, Ile-9, and Val-13 constitute the hydrophobic face of the *N*-terminal region.

Acknowledgements

This work was supported by grants from the National Science Council, R. O. C. (to L.S. Chang) NSC95-2320-B110-007-MY3, and the National Sun Yat-Sen University-Kaohsiung Medical University Joint Center.

REFERENCES

1. Kini RM. Phospholipase A_2, a complex multifunctional protein puzzle. In *Venom Phospholipase A_2 Enzymes: Structure, Function and Mechanism*, Kini RM (ed.). John Wiley and Son: Chichester, 1997; 1–28.
2. Qin S, Pande AH, Nemec KN, He XM, Tatulian SA. Evidence for the regulatory role of the N-terminal helix of secretory phospholipase A_2 from studies on native and chimeric proteins. *J. Biol. Chem.* 2005; **280**: 36 773–36 783.
3. Qin S, Pande AH, Nemec KN, Tatulian SA. The N-terminal α-helix of pancreatic phospholipase A_2 determines productive-mode orientation of the enzyme at the membrane surface. *J. Mol. Biol.* 2004; **344**: 71–89.
4. Tatulian SA. Structural effects of covalent inhibition of phospholipase A_2 suggest allosteric coupling between membrane binding and catalytic sites. *Biophys. J.* 2003; **84**: 1773–1783.
5. Scott DL, White SP, Otwinowski Z, Yuan W, Gelb MH, Sigler PB. Interfacial catalysis: the mechanism of phospholipase A_2. *Science* 1990; **250**: 1541–1546.
6. White SP, Scott DL, Otwinowski Z, Gelb MH, Sigler PB. Crystal structure of cobra-venom phospholipase A_2 in a complex with a transition-state analogue. *Science* 1990; **250**: 1560–1563.
7. Chang LS, Cheng YC, Chen CP. Modification of Lys-6 and Lys-65 affects the structural stability of Taiwan cobra phospholipase A_2. *Protein J.* 2006; **25**: 127–134.
8. Renetseder R, Dijkstra BW, Huizinga K, Kalk KH, Drenth J. Crystal structure of bovine pancreatic phospholipase A_2 covalently

inhibited by *p*-bromo-phenacyl-bromide. *J. Mol. Biol.* 1988; **200**: 181–188.
9. Zhao H, Tang L, Wang X, Zhou Y, Lin Z. Structure of a snake venom phospholipase A_2 modified by *p*-bromo-phenacyl-bromide. *Toxicon* 1998; **36**: 875–886.
10. Andersson T, Drakenberg T, Forsen S, Wieloch T, Lindstrom M. Calcium binding to porcine pancreatic prophospholipase A_2 studied by ^{43}Ca NMR. *FEBS Lett.* 1981; **123**: 115–117.
11. Chang LS, Lin SR, Chang CC. The essentiality of calcium ion in the enzymatic activity of Taiwan cobra phospholipase A_2. *J. Protein Chem.* 1996; **15**: 701–707.
12. Chang LS, Lin SR, Chang CC. Identification of Arg-30 as the essential residue for the enzymatic activity of Taiwan cobra phospholipase A_2. *J. Biochem. (Tokyo)* 1998; **124**: 764–768.
13. Thannhauser TW, Scheraga HA. Reversible blocking of half-cystine residues of proteins and an irreversible specific deamidation of asparagine-67 of S-sulforibonuclease under mild conditions. *Biochemistry* 1985; **24**: 7681–7688.
14. Chang LS, Wu PF, Lin J. cDNA sequence analysis and expression of cardiotoxins from Taiwan Cobra. *Biochem. Biophys. Res. Commun.* 1996; **219**: 116–121.
15. Chang LS, Wu PF, Chang CC. Expression of Taiwan banded krait phospholipase A_2 in *Escherichia coli*, a fully active enzyme generated by hydrolyzing with aminopeptidase. *Biochem. Biophys. Res. Commun.* 1996; **225**: 990–996.
16. Eftink MR, Ghiron CA. Fluorescence quenching studies with proteins. *Anal. Biochem.* 1981; **114**: 199–227.
17. Chang LS, Wen EY, Hung JJ, Chang CC. Energy transfer from tryptophan residues of proteins to 8-anilinonaphthalene-1-sulfonate. *J. Protein Chem.* 1994; **13**: 635–640.
18. Chang LS, Kuo KW, Chang CC. Identification of functional involvement of tryptophan residues in phospholipase A_2 from *Naja naja atra* (Taiwan cobra) snake venom. *Biochim. Biophys. Acta* 1993; **1202**: 216–220.
19. Sumandea M, Das S, Sumandea C, Cho W. Roles of aromatic residues in high interfacial activity of *Naja naja atra* phospholipase A_2. *Biochemistry* 1999; **38**: 16 290–16 297.
20. Cardamone M, Puri NK. Spectrofluorimetric assessment of the surface hydrophobicity of proteins. *Biochem. J.* 1992; **282**: 589–593.
21. Jones BE, Jennings PA, Pierre RA, Mattews CR. Development of nonpolar surfaces in the folding of Escherichia coli dihydrofolate reductase detected by 1-anilinonaphthalene-8-sulfonate binding. *Biochemistry* 1994; **33**: 15 250–15 258.
22. Stryer L. Fluorescence spectroscopy of proteins. *Science* 1968; **162**: 526–533.
23. Yang CC, Chang LS. Role of the N-terminal region in phospholipases A_2 from *Naja naja atra* (Taiwan cobra) and *Naja nigricollis* (spitting cobra) venoms. *Toxicon* 1988; **26**: 721–731.
24. Yang CC, King K, Sun TP. Chemical modification of lysine and histidine residues in phospholipase A_2 from the venom of *Naja naja atra* (Taiwan cobra). *Toxicon* 1981; **19**: 645–659.
25. Campbell ID, Dwek RA. *Biological Spectroscopy*. The Benjamin/Cummings Publishing Company Inc: Menlo park, CA, 1984; 91–126.
26. Lakowicz JR. *Principles of Fluorescence Spectroscopy*. Kluwer Academic/Plenum Publishers: New York, 1999.
27. Chang LS, Lin SR, Chang CC. Probing calcium ion-induced conformational changes of Taiwan cobra phospholipase A_2 by trinitrophenylation of lysine residues. *J. Protein Chem.* 1997; **16**: 51–57.
28. Marki F, Hanulak V. Recombinant human synovial fluid phospholipase A_2 and N-terminal variant: kinetic parameters and response to inhibitors. *J. Biochem. (Tokyo)* 1993; **113**: 734–737.
29. Liu X, Zhu H, Huang B, Rogers J, Yu BZ, Kumar A, Jain MK, Sundaralingam M, Tsai MD. Phospholipase A_2 engineering. Probing the structural and functional roles of N-terminal residues with site-directed mutagenesis, X-ray, and NMR. *Biochemistry* 1995; **34**: 7322–7334.
30. Pande AH, Qin S, Nemec KN, He XM, Tatulian SA. Isoform-specific membrane insertion of secretory phospholipase A_2 and functional implications. *Biochemistry* 2006; **45**: 12 436–12 447.

DOI: 10.1002/psc